

## Substrate Affinity of Photosensitizers Derived from Chlorophyll-a: The ABCG2 Transporter Affects the Phototoxic Response of Side Population Stem Cell-like Cancer Cells to Photodynamic Therapy

Janet Morgan,\* Jennifer D. Jackson, Xiang Zheng, Suresh K. Pandey, and Ravindra K. Pandey

*Department of Dermatology and Department of Cell Stress Biology, Roswell Park Cancer Institute, Buffalo, New York 14263*

Received May 6, 2010; Revised Manuscript Received July 20, 2010; Accepted August 4, 2010

**Abstract:** Photosensitizers (PS) synthesized with the aim of optimizing photodynamic therapy (PDT) of tumors do not always fulfill their potential when tested *in vitro* and *in vivo* in different tumor models. The ATP-dependent transporter ABCG2, a multidrug resistant pump expressed at variable levels in cancerous cells, can bind and efflux a wide range of structurally different classes of compounds including several PS used preclinically and clinically such as porphyrins and chlorins. ABCG2 may lower intracellular levels of substrate PS below the threshold for cell death in tumors treated by PDT, leaving resistant cells to repopulate the tumor. To determine some of the structural factors that affect substrate affinity of PS for ABCG2, we used an ABCG2-expressing cell line (HEK 293 482R) and its nonexpressing counterpart, and tyrosine kinase ABCG2 inhibitors in a simple flow cytometric assay to identify PS effluxed by the ABCG2 pump. We tested a series of conjugates of substrate PS with different groups attached at different positions on the tetrapyrrole macrocycle to examine whether a change in affinity for the pump occurred and whether such changes depended on the position or the structure/type of the attached group. PS without substitutions including pyropheophorbides and purpurinimides were generally substrates for ABCG2, but carbohydrate groups conjugated at positions 8, 12, 13, and 17 but not at position 3 abrogated ABCG2 affinity regardless of structure or linking moiety. At position 3, affinity was retained with the addition of iodobenzene, alkyl chains and monosaccharides, but not with disaccharides. This suggests that structural characteristics at position 3 may offer important contributions to requirements for binding to ABCG2. We examined several tumor cell lines for ABCG2 activity, and found that although some cell lines had negligible ABCG2 activity in bulk, they contained a small ABCG2-expressing side population (SP) thought to contain cells which are responsible for initiating tumor regrowth. We examined the relevance of the SP to PDT resistance with ABCG2 substrates *in vitro* and *in vivo* in the murine mammary tumor 4T1. We show for the first time *in vivo* that the substrate PS HPPH (2-[1-hexyloxyethyl]-2-devinyl pyropheophorbide-a) but not the nonsubstrate PS HPPH-Gal (a galactose conjugate of HPPH) selectively preserved the SP which was primarily responsible for regrowth *in vitro*. The SP could be targeted by addition of imatinib mesylate, a tyrosine kinase inhibitor which inhibits the ATPase activity of ABCG2, and prevents efflux of substrates. A PDT resistant SP may be responsible for recurrences observed both preclinically and clinically. To prevent ABCG2 mediated resistance, choosing nonsubstrate PS or administering an ABCG2 inhibitor alongside a substrate PS might be advantageous when treating ABCG2-expressing tumors with PDT.

**Keywords:** ABCG2; cancer stem cells; HPPH; photodynamic therapy; photosensitizer; resistance; side population; tetrapyrrole; tyrosine kinase inhibitor

## Introduction

Our group is focused on designing, synthesizing and evaluating photosensitizers (PS) for enhanced photodynamic therapy (PDT) and multifunctional photosensitizer-based agents ultimately for clinical fluorescence, PET and MRI imaging, by the addition of various suitable moieties to photosensitive molecules.<sup>1–5</sup> To evaluate the newly synthesized compounds we use ostensibly standard murine tumor models such as the radiation induced fibrosarcoma (RIF-1) and colon adenocarcinoma Colon26 for comparisons with previous PS.<sup>6–9</sup> However, in light of research suggesting that ATP-dependent transporters including the G subclass (ABCG2) are expressed at varying levels on tumors, use of

certain tumor models may present drawbacks for testing PS efficacy. Recent work indicates that many photosensitizers (PS) used in clinical and preclinical photodynamic therapy (PDT) are substrates for the ATP-dependent transporter ABCG2, including HPPH (Photochlor), benzporphyrin derivative (BPD, Verteporfin), Hypericin and protoporphyrin IX (following exogenous administration of ALA).<sup>10–13</sup> These and similar porphyrins and chlorin photosensitizers, including some studied in this work (Figure 1 in the Supporting Information), were not substrates of other commonly expressed ABC transporters ABCC1 (MRP1) and ABCB1 (Pgp).<sup>11,14–18</sup> ABCG2, like other members of the ATP-binding cassette family transporters, binds and transports a wide range of substrates within and out of cells. When ABCG2 is expressed in the cell membrane of certain types of normal cells, it prevents accumulation of exogenous or endogenous compounds which may be detrimental to cell

\* To whom correspondence should be addressed: Janet Morgan, Department of Dermatology, Roswell Park Cancer Institute, Buffalo, NY 14222. Phone: 716 845 3371. Fax: 716 845 2364. E-mail: janet.morgan@roswellpark.org.

- (1) Pandey, S. K.; Gryshuk, A. L.; Sajjad, M.; Zheng, X.; Chen, Y.; Abouzeid, M. M.; Morgan, J.; Charamisinau, I.; Nabi, H. A.; Oseroff, A.; Pandey, R. K. Multimodality agents for tumor imaging (PET, fluorescence) and photodynamic therapy. A possible “see and treat” approach. *J. Med. Chem.* **2005**, *48*, 6286–6295.
- (2) Li, G.; Slansky, A.; Dobhal, M. P.; Goswami, L. N.; Graham, A.; Chen, Y.; Kanter, P.; Alberico, R. A.; Sperryak, J.; Morgan, J.; Mazurchuk, R.; Oseroff, A.; Grossman, Z.; Pandey, R. K. Chlorophyll-a analogues conjugated with aminobenzyl-DTPA as potential bifunctional agents for magnetic resonance imaging and photodynamic therapy. *Bioconjugate Chem.* **2005**, *16*, 32–42.
- (3) Chen, Y.; Gryshuk, A.; Achilefu, S.; Ohulchansky, T.; Potter, W.; Zhong, T.; Morgan, J.; Chance, B.; Prasad, P. N.; Henderson, B. W.; Oseroff, A.; Pandey, R. K. A novel approach to a bifunctional photosensitizer for tumor imaging and phototherapy. *Bioconjugate Chem.* **2005**, *16*, 1264–1274.
- (4) Pandey, S. K.; Sajjad, M.; Chen, Y.; Pandey, A.; Missert, J. R.; Batt, C.; Yao, R.; Nabi, H. A.; Oseroff, A. R.; Pandey, R. K. Compared to purpurinimides, the pyropheophorbide containing an iodobenzyl group showed enhanced PDT efficacy and tumor imaging (124I-PET) ability. *Bioconjugate Chem.* **2009**, *20*, 274–282.
- (5) Pandey, S. K.; Sajjad, M.; Chen, Y.; Zheng, X.; Yao, R.; Missert, J. R.; Batt, C.; Nabi, H. A.; Oseroff, A. R.; Pandey, R. K. Comparative positron-emission tomography (PET) imaging and phototherapeutic potential of <sup>124</sup>I- labeled methyl methyl- 3-(1'-iodobenzyl)pyropheophorbide-a vs the corresponding glucose and galactose conjugates. *J. Med. Chem.* **2009**, *52*, 445–455.
- (6) Henderson, B. W.; Waldow, S. M.; Mang, T. S.; Potter, W. R.; Malone, P. B.; Dougherty, T. J. Tumor destruction and kinetics of tumor cell death in two experimental mouse tumors following photodynamic therapy. *Cancer Res.* **1985**, *45*, 572–576.
- (7) Bellnier, D. A.; Henderson, B. W.; Pandey, R. K.; Potter, W. R.; Dougherty, T. J. Murine pharmacokinetics and antitumor efficacy of the photodynamic sensitizer 2-[1-hexyloxyethyl]-2-devinyl pyropheophorbide-a. *J. Photochem. Photobiol., B* **1993**, *20*, 55–61.
- (8) Pandey, R. K.; Sumlin, A. B.; Constantine, S.; Aoudla, M.; Potter, W. R.; Bellnier, D. A.; Henderson, B. W.; Rodgers, M. A.; Smith, K. M.; Dougherty, T. J. Alkyl ether analogs of chlorophyll-a derivatives: Part 1. Synthesis, photophysical properties and photodynamic efficacy. *Photochem. Photobiol.* **1996**, *64*, 194–204.
- (9) Henderson, B. W.; Gollnick, S. O.; Snyder, J. W.; Busch, T. M.; Kousis, P. C.; Cheney, R. T.; Morgan, J. Choice of oxygen-conserving treatment regimen determines the inflammatory response and outcome of photodynamic therapy of tumors. *Cancer Res.* **2004**, *64*, 2120–2126.
- (10) Jonker, J. W.; Buitelaar, M.; Wagenaar, E.; van, d. V.; Scheffer, G. L.; Scheper, R. J.; Plosch, T.; Kuipers, F.; Elferink, R. P.; Rosing, H.; Beijnen, J. H.; Schinkel, A. H. The breast cancer resistance protein protects against a major chlorophyll-derived dietary phototoxin and protoporphyrin. *Proc. Natl. Acad. Sci. U.S.A.* **2002**, *99*, 15649–15654.
- (11) Robey, R. W.; Steadman, K.; Polgar, O.; Bates, S. E. ABCG2-mediated transport of photosensitizers: potential impact on photodynamic therapy. *Cancer Biol. Ther.* **2005**, *4*, 187–194.
- (12) Liu, W.; Baer, M. R.; Bowman, M. J.; Pera, P.; Zheng, X.; Morgan, J.; Pandey, R. A.; Oseroff, A. R. The tyrosine kinase inhibitor imatinib mesylate enhances the efficacy of photodynamic therapy by inhibiting ABCG2. *Clin. Cancer Res.* **2007**, *13*, 2463–2470.
- (13) Morgan, J.; Petrucci, C. M. The effect of ALA/PpIX PDT on putative cancer stem cells in tumorside populations. Kessel, D. H. 738011 [Photodynamic Therapy: Back to the future], 1–9. 2009. SPIE. SPIE Proceedings. 6–11–2009.
- (14) Li, W.; Zhang, W. J.; Ohnishi, K.; Yamada, I.; Ohno, R.; Hashimoto, K. 5-Aminolaevulinic acid-mediated photodynamic therapy in multidrug resistant leukemia cells. *J. Photochem. Photobiol., B* **2001**, *60*, 79–86.
- (15) Teiten, M. H.; Bezdetnaya, L.; Merlin, J. L.; Bour-Dill, C.; Pauly, M. E.; Dicato, M.; Guillemin, F. Effect of meta-tetra(hydroxyphenyl)chlorin (mTHPC)-mediated photodynamic therapy on sensitive and multidrug-resistant human breast cancer cells. *J. Photochem. Photobiol., B* **2001**, *62*, 146–152.
- (16) Merlin, J. L.; Gautier, H.; Barberi-Heyob, M.; Teiten, M. H.; Guillemin, F. The multidrug resistance modulator SDZ-PSC 833 potentiates the photodynamic activity of chlorin e6 independently of P-glycoprotein in multidrug resistant human breast adenocarcinoma cells. *Int. J. Oncol.* **2003**, *22*, 733–739.
- (17) Tsai, T.; Hong, R. L.; Tsai, J. C.; Lou, P. J.; Ling, I. F.; Chen, C. T. Effect of 5-aminolaevulinic acid-mediated photodynamic therapy on MCF-7 and MCF-7/ADR cells. *Lasers Surg. Med.* **2004**, *34*, 62–72.
- (18) Robey, R. W.; Steadman, K.; Polgar, O.; Morisaki, K.; Blayney, M.; Mistry, P.; Bates, S. E. Pheophorbide a is a specific probe for ABCG2 function and inhibition. *Cancer Res.* **2004**, *64*, 1242–1246.

vitality, homeostasis or development, such as toxins, heme precursors or steroids and their metabolites.<sup>19–21</sup>

Many tumor cells also express ABCG2 in their cell membranes, where it can function as a multidrug resistance protein, effluxing certain substrate chemotherapeutic agents and decreasing the clinical response.<sup>19,22–25</sup> Thus, substrate PS used in the treatment of cancer with PDT can be effluxed from ABCG2-expressing cells, decreasing the intracellular PS concentration and possibly lowering the level below the threshold required to produce a phototoxic response. The quest for a new generation of more selective and effective PS has led to studies in which modifications to PS have been examined in structure activity relationships (SAR). However, interpretation of phototoxic efficacy in a SAR study performed in tumors expressing ABCG2 may confound what should be straightforward associations if the structural changes convert a substrate PS to a nonsubstrate PS or *vice versa*. Alternatively, activity of ABCG2 could help to explain what might appear to be aberrant exceptions to otherwise rational relationships between structural changes and phototoxicity.<sup>26</sup>

Thus far, choices of photosensitizers used for PDT have not been defined on the basis of specificity or affinity for ABCG2, nor have *in vitro* and *in vivo* cancer models for PDT been chosen because of ABCG2 expression or lack thereof. Indeed, many tumors do not appear to express large

amounts of ABCG2, or if they do it is not necessarily present in the cell membrane where it functions as an effluxing pump, but in the cytoplasm or nucleus,<sup>27</sup> in this study and our own unpublished observations. However, it has become evident that a small subset of ABCG2-expressing cells known as a side population (SP) is present in most types of tissues<sup>28</sup> and in many tumors, and possesses stem cell-like characteristics.<sup>29</sup> The SP was originally identified by flow cytometry as a subset of bone marrow cells which excluded the fluorescent dye Hoechst 33342.<sup>30</sup> ABCG2 was determined to be primarily responsible for the low accumulation of Hoechst in the SP.<sup>29,31</sup> In many tumors, the SP has been demonstrated as enriched for cells with enhanced tumorigenic potential, known as tumor initiating cells (TIC), stem cell-like cancer cells (SCLCC) or cancer stem cells (CSC). The TIC or CSC have been postulated as the source and driving force of tumor growth and development.<sup>32</sup> If the (usually) small number of SP cells present in tumors exclude ABCG2 substrate PS and evade PDT-mediated death, they could be responsible for repopulating tumors, causing recurrences and diminished clinical outcome.

We have previously tested analogues of chlorins derived from chlorophyll-a in which structures were modified with various substituents at different peripheral positions in *in vitro* and *in vivo* SAR studies for PDT activity.<sup>4,26,33–37</sup> This was successful in identifying efficient photosensitizers with

- (19) Zhou, S.; Schuetz, J. D.; Bunting, K. D.; Colapietro, A. M.; Sampath, J.; Morris, J. J.; Lagutina, I.; Grosveld, G. C.; Osawa, M.; Nakauchi, H.; Sorrentino, B. P. The ABC transporter Bcrp1/ABCG2 is expressed in a wide variety of stem cells and is a molecular determinant of the side-population phenotype. *Nat. Med.* **2001**, *7*, 1028–1034.
- (20) Suzuki, M.; Suzuki, H.; Sugimoto, Y.; Sugiyama, Y. ABCG2 transports sulfated conjugates of steroids and xenobiotics. *J. Biol. Chem.* **2003**, *278*, 22644–22649.
- (21) Fetsch, P. A.; Abati, A.; Litman, T.; Morisaki, K.; Honjo, Y.; Mittal, K.; Bates, S. E. Localization of the ABCG2 mitoxantrone resistance-associated protein in normal tissues. *Cancer Lett.* **2006**, *235*, 84–92.
- (22) Rajendra, R.; Gounder, M. K.; Saleem, A.; Schellens, J. H.; Ross, D. D.; Bates, S. E.; Sinko, P.; Rubin, E. H. Differential effects of the breast cancer resistance protein on the cellular accumulation and cytotoxicity of 9-aminocamptothecin and 9-nitrocamptothecin. *Cancer Res.* **2003**, *63*, 3228–3233.
- (23) Yang, C. H.; Chen, Y. C.; Kuo, M. L. Novobiocin sensitizes BCRP/MXR/ABCP overexpressing topotecan-resistant human breast carcinoma cells to topotecan and mitoxantrone. *Anticancer Res.* **2003**, *23*, 2519–2523.
- (24) Robey, R. W.; Polgar, O.; Deeken, J.; To, K. W.; Bates, S. E. ABCG2: determining its relevance in clinical drug resistance. *Cancer Metastasis Rev.* **2007**, *26*, 39–57.
- (25) Polgar, O.; Robey, R. W.; Bates, S. E. ABCG2: structure, function and role in drug response. *Expert Opin. Drug Metab. Toxicol.* **2008**, *4*, 1–15.
- (26) Zheng, X.; Morgan, J.; Pandey, S. K.; Chen, Y.; Tracy, E.; Baumann, H.; Missert, J. R.; Batt, C.; Jackson, J.; Bellnier, D. A.; Henderson, B. W.; Pandey, R. K. Conjugation of 2-(1'-Hexyloxyethyl)-2-devinylpyropheophorbide-a (HPPH) to carbohydrates changes its subcellular distribution and enhances photodynamic activity in vivo. *J. Med. Chem.* **2009**, *52*, 4306–4318.
- (27) Chen, J. S.; Pardo, F. S.; Wang-Rodriguez, J.; Chu, T. S.; Lopez, J. P.; Aguilera, J.; Altuna, X.; Weisman, R. A.; Ongkeko, W. M. EGFR regulates the side population in head and neck squamous cell carcinoma. *Laryngoscope* **2006**, *116*, 401–406.
- (28) Hirschmann-Jax, C.; Foster, A. E.; Wulf, G. G.; Nuchtern, J. G.; Jax, T. W.; Gobel, U.; Goodell, M. A.; Brenner, M. K. A distinct “side population” of cells with high drug efflux capacity in human tumor cells. *Proc. Natl. Acad. Sci. U. S. A* **2004**, *101*, 14228–14233.
- (29) Patrawala, L.; Calhoun, T.; Schneider-Broussard, R.; Zhou, J.; Claypool, K.; Tang, D. G. Side population is enriched in tumorigenic, stem-like cancer cells, whereas ABCG2+ and ABCG2–cells are similarly tumorigenic. *Cancer Res.* **2005**, *65*, 6207–6219.
- (30) Goodell, M. A.; Brose, K.; Paradis, G.; Conner, A. S.; Mulligan, R. C. Isolation and functional properties of murine hematopoietic stem cells that are replicating in vivo. *J. Exp. Med.* **1996**, *183*, 1797–1806.
- (31) Zhou, S.; Morris, J. J.; Barnes, Y.; Lan, L.; Schuetz, J. D.; Sorrentino, B. P. Bcrp1 gene expression is required for normal numbers of side population stem cells in mice, and confers relative protection to mitoxantrone in hematopoietic cells in vivo. *Proc. Natl. Acad. Sci. U. S. A* **2002**, *99*, 12339–12344.
- (32) Reya, T.; Morrison, S. J.; Clarke, M. F.; Weissman, I. L. Stem cells, cancer, and cancer stem cells. *Nature* **2001**, *414*, 105–111.
- (33) Pandey, R. K.; Shiau, F.-Y.; Sumlin, A. B.; Dougherty, T. J.; Smith, K. M. Structure activity relationships among photosensitizers related to pheophorbides and bacteriopheophorbides. *Bioorg. Med. Chem. Lett.* **1992**, *2*, 491–496.
- (34) Henderson, B. W.; Bellnier, D. A.; Greco, W. R.; Sharma, A.; Pandey, R. K.; Vaughan, L. A.; Weishaupt, K. R.; Dougherty, T. J. An in vivo quantitative structure-activity relationship for a congeneric series of pyropheophorbide derivatives as photosensitizers for photodynamic therapy. *Cancer Res.* **1997**, *57*, 4000–4007.



good tumor uptake and PDT efficacy. However, depending on the structural modifications made, the effects did not always translate with similar efficacy into different tumor models. We discovered that some of the tumor models expressed different levels of ABCG2 and that some of the structural modifications of the analogues changed their affinity for or were no longer transported by ABCG2; for example addition of galactose to HPPH produced a nonsubstrate.<sup>12,26</sup> Thus, a nonsubstrate might be more effective than a substrate in a model in which ABCG2 was expressed at high levels, due partly to increased intracellular levels of PS; whereas it might be equally, less, or more effective in a low or non-ABCG2-expressing model depending on other properties of the PS or the tumor model.<sup>12,26</sup>

Identifying which tumor models express functional ABCG2 and which newly synthesized photosensitizers are ABCG2 substrates is essential for interpreting PDT efficacy, and choosing suitable photosensitizers for subsequent clinical use as PDT and imaging agents.

In this study we examined the role that different substituents and their positions on the macrocycle of different chlorins imposed on their affinity for the ABCG2 transporter, to determine factors that might improve accumulation and phototoxicity in ABCG2-expressing cells. We then tested the hypothesis that PDT using substrate and nonsubstrate PS had differential phototoxic effects *in vitro* and *in vivo* on the SP of 4T1, an immunocompetent murine mammary cancer model.<sup>38</sup> The SP in 4T1 was found to express a stem cell-like phenotype, was more tumorigenic and chemoresistant than the NON-SP, and was more efficient at reconstituting the full tumor phenotype than the NON-SP. The SP was therefore described as containing stem cell-like cancer cells (SCLCC).<sup>38</sup> The SP should be relatively resistant to a substrate PS compared to a nonsubstrate PS because it will be pumped out by ABCG2.

We previously found that conjugating galactose and other carbohydrates to HPPH at position 17 on the macrocycle

prevented the HPPH from being transported out of cells by ABCG2.<sup>12,26</sup> To determine whether such modifications were unique to HPPH or could be extrapolated to other positions and series of photosensitizer analogues we examined here the effects on ABCG2-mediated transport of different substituents conjugated at various peripheral positions on different chlorins.

We used a simple and flexible *in vitro* flow cytometry based test to measure the relative fluorescence of photosensitizer accumulation in the presence or absence of ABCG2 inhibitors in cells expressing or not expressing ABCG2 to determine whether modifications to substrate photosensitizers affected their affinity for the ABCG2 transporter. In a similar manner we also measured ABCG2 activity using HPPH as a substrate (with and without ABCG2 inhibitors) in several types of tumor cells to determine whether they expressed appreciable levels of functional ABCG2, and consequently were likely to be less vulnerable to PDT.

## Experimental Section

**Cells and Culture Conditions.** Cells were cultured in medium supplemented with 10% FCS, 2 mM L-glutamine, penicillin (10 IU/mL) and streptomycin (10 µg/mL) at 37 °C in 95% air 5% CO<sub>2</sub> in a humidified atmosphere and were harvested in log phase of growth at 70–90% confluency. The ABCG2-expressing (HEK-293 482R) and ABCG2 negative (HEK-293 PcDNA) derivatives of HEK-293 (transformed human embryonic kidney) cells<sup>39</sup> were used to screen PS for substrate specificity and affinity for the ABCG2 transporter. HEK-293 cells were grown in DMEM selection medium additionally supplemented with 2 mg/mL G418 sulfate (Mediatech, Inc., Manassas, VA).

Relative ABCG2 activity was measured in several cell lines (American Type Culture Collection (ATCC) Manassas, VA) used in our laboratories for examining PDT mechanisms and efficacy. They included A549 (human non small cell lung carcinoma), HeLa (human cervical adenocarcinoma), FaDu (human hypopharyngeal squamous cell carcinoma), U87MG (human glioblastoma multiforme), Colon26 (murine colon carcinoma) and RIF-1 (murine radiation induced fibrosarcoma). The cell lines were chosen to demonstrate different aspects of the role of ABCG2 in tumor models treated with PDT. The cell lines RIF-1 and Colon26A, cell lines used frequently by us as *in vitro* and *in vivo* screening models for PDT, recently were found to express ABCG2 by Western blot and have moderate and low levels respectively of functional ABCG2.<sup>12</sup> Colon26A has been adapted to *in vitro* growth whereas Colon26B passaged *in vivo* and grown for only a few passages *in vitro* does not express detectable ABCG2 by Western blot.<sup>26</sup> FaDu has no detectable ABCG2 by Western blot.<sup>12</sup> A549 was reported elsewhere to have

- (35) Potter, W. R.; Henderson, B. W.; Bellnier, D. A.; Pandey, R. K.; Vaughan, L. A.; Weishaupt, K. R.; Dougherty, T. J. Parabolic Quantitative Structure-Activity Relationships and Photodynamic Therapy: Application of a three-compartment model with clearance to the *in vivo* quantitative structure-activity relationships of a congeneric series of pyropheophorbide derivatives used as photosensitizers for photodynamic therapy. *Photochem. Photobiol.* **1999**, *70*, 781–788.
- (36) Pandey, S. K.; Zheng, X.; Morgan, J.; Missert, J. R.; Liu, T. H.; Shibata, M.; Bellnier, D. A.; Oseroff, A. R.; Henderson, B. W.; Dougherty, T. J.; Pandey, R. K. Purpurinimide carbohydrate conjugates: effect of the position of the carbohydrate moiety in photosensitizing efficacy. *Mol. Pharm.* **2007**, *4*, 448–464.
- (37) Gryshuk, A.; Chen, Y.; Goswami, L. N.; Pandey, S.; Missert, J. R.; Ohulchanskyy, T.; Potter, W.; Prasad, P. N.; Oseroff, A.; Pandey, R. K. Structure-activity relationship among purpurinimides and bacteriopurpurinimides: trifluoromethyl substituent enhanced the photosensitizing efficacy. *J. Med. Chem.* **2007**, *50*, 1754–1767.
- (38) Kruger, J. A.; Kaplan, C. D.; Luo, Y.; Zhou, H.; Markowitz, D.; Xiang, R.; Reisfeld, R. A. Characterization of stem cell-like cancer cells in immune-competent mice. *Blood* **2006**, *108*, 3906–3912.

- (39) Robey, R. W.; Honjo, Y.; Morisaki, K.; Nadjem, T. A.; Runge, S.; Risbood, M.; Poruchynsky, M. S.; Bates, S. E. Mutations at amino-acid 482 in the ABCG2 gene affect substrate and antagonist specificity. *Br. J. Cancer* **2003**, *89*, 1971–1978.

functional ABCG2.<sup>40</sup> HeLa cell lines were represented by low passage HeLa– (ABCG2 negative) and high passage HeLa+ (ABCG2 positive) cells. RIF-1 cells were grown in alpha-MEM; A549, HeLa and Colon26 were grown in RPMI-1640, FaDu was grown in EMEM additionally supplemented with 1 mM sodium pyruvate and nonessential amino acids and U87 was grown in DMEM with 1 mM sodium pyruvate.

To test the relevance of PDT on the ABCG2-expressing SP of a tumor model *in vitro* and *in vivo* we treated 4T1 murine mammary adenocarcinoma, reported as having a SP<sup>38</sup> with HPPH or HPPH-Gal PDT as the representative substrate and nonsubstrate PS respectively. 4T1 (CRL-2539, ATCC, Manassas, VA) was grown in RPMI-1640 supplemented with 10% FCS, L-glutamine, penicillin and streptomycin.

**ABCG2 Inhibitors and Chemicals.** Fumitremorgin C (FTC) (Alexis Biochemicals) was dissolved in DMSO to 5 mM and stored at 4 °C. Imatinib mesylate (IM) (Novartis Pharmaceuticals, Basel Switzerland) was dissolved in water to 11.3 mM and stored at 4 °C. Dye Cycle Violet (DCV) as supplied, 5 mM in water and 7-amino actinomycin D (7-AAD) 1 mg/mL in 5% methanol in water, were purchased from Invitrogen and stored at 4 °C. Reagents were brought to room temperature before use. Pheophorbide-a (PhA) was purchased from Frontier Scientific, Logan, UT, dissolved in DMSO to 5 mM and stored at ambient temperature.

**Flow Cytometry for Testing Substrate Specificity and Affinity.** Cells were harvested with trypsin, filtered through 30  $\mu$ m mesh to remove aggregates and obtain a single cell suspension, and then counted and suspended at  $10^6$  mL<sup>-1</sup> in growth medium containing 2% FCS. Cells (0.5 mL) were aliquoted in triplicate sets into 5 mL flow cytometry tubes (BD Invitrogen). Vehicle or tyrosine kinase inhibitors (TKI) of ABCG2, IM at 10  $\mu$ M or FTC at 15 or 20  $\mu$ M were added to tubes and incubated for 30 min at 37 °C. The PS (1  $\mu$ M) were then added to tubes and incubated for a further 60 min at 37 °C, with occasional mixing (every 15 min). Control tubes contained cells only, vehicle only, IM only or FTC only. Tubes were then placed on ice, to inhibit ATP-dependent efflux activity, and immediately analyzed by flow cytometry. Preliminary experiments used pheophorbide-a (PhA), a strongly effluxed substrate of ABCG2,<sup>18</sup> as a control to demonstrate that the assay functioned properly and to provide a standard for comparison of the relative substrate affinity of the tested compounds. Subsequently we used pyropheophorbide-a (PPA) as the reference control each time a series of PS was assayed, with similar results to PhA. Initially we tested FTC as the ABCG2 inhibitor, which has been described as specific for ABCG2,<sup>41,42</sup> but we found that higher concentrations (15–20  $\mu$ M) were needed for

consistent inhibition than reported elsewhere (10  $\mu$ M), and also caused some dark toxicity. The majority of the experiments were therefore performed using IM at 10  $\mu$ M as the inhibitor, which behaved consistently and did not cause observable toxicity at the short incubation times used.<sup>12</sup>

Cellular fluorescence was measured by flow cytometry using CellQuest to acquire 10,000 events. Depending on the specific fluorescence profile of the photosensitizer we primarily used the FACSCalibur flow cytometer (Beckton and Dickinson) with laser excitation at 488 or 635 nm, and emission at >670 nm or 661/16 nm respectively, or the LSR II flow cytometer with laser excitation at 405 nm and emission at >645 nm for longer wavelength-emitting photosensitizers (purpurinimides in this study). Data was analyzed by FCS Express (DeNovo Software, Los Angeles, CA). Histograms of fluorescence were generated for all samples, the autofluorescence of cell samples without photosensitizer was subtracted and the fractional change in fluorescence in the cells due to the PS caused by the presence of the inhibitor relative to its absence was calculated.

If a significant difference was observed in the fluorescence exhibited by the ABCG2+ HEK-293 482R cells in the presence of the inhibitor, then the PS was considered a substrate. If there was no difference in the fluorescence exhibited in the presence of the inhibitor, then the PS was considered a nonsubstrate. Significance was based on differences between the means of samples (from at least 3 experiments with triplicate samples) with and without inhibitor, analyzed by paired 2-tailed *t* tests, and greater fluorescence increases indicated higher affinity. Mean changes of less than approximately 0.10–0.15 were generally found to be insignificant. No difference in fluorescence should be observed in the ABCG2– control HEK-293 PcDNA cells since no ABCG2 is present for pump activity or its inhibition.

**Photosensitizers.** The photosensitizers are grouped as derivatives related to pyropheophorbide-a, to HPPH (2-(1'-hexyloxyethyl) pyropheophorbide-a) and to purpurinimides as shown and numbered (#) in Charts 1–4. All PS were synthesized at Roswell Park Cancer Institute, and their structures and photosensitizing efficacy have been published previously.<sup>1,2,8,26,36,43</sup> PS were dissolved in 1% Tween 80 in 5% dextrose (D5W) and stored at 4 °C. Final Tween 80 levels were less than 0.02%.

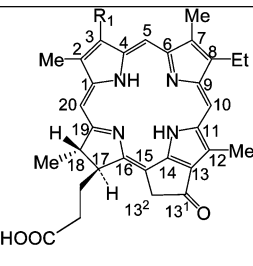
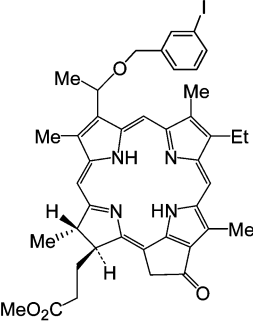
(40) Sung, J. M.; Cho, H. J.; Yi, H.; Lee, C. H.; Kim, H. S.; Kim, D. K.; bd El-Aty, A. M.; Kim, J. S.; Landowski, C. P.; Hediger, M. A.; Shin, H. C. Characterization of a stem cell population in lung cancer A549 cells. *Biochem. Biophys. Res. Commun.* **2008**, *371*, 163–167.

(41) Rabindran, S. K.; He, H.; Singh, M.; Brown, E.; Collins, K. I.; Annable, T.; Greenberger, L. M. Reversal of a novel multidrug resistance mechanism in human colon carcinoma cells by fumitremorgin C. *Cancer Res.* **1998**, *58*, 5850–5858.

(42) Rabindran, S. K.; Ross, D. D.; Doyle, L. A.; Yang, W.; Greenberger, L. M. Fumitremorgin C reverses multidrug resistance in cells transfected with the breast cancer resistance protein. *Cancer Res.* **2000**, *60*, 47–50.

(43) Zheng, G.; Graham, A.; Shibata, M.; Missert, J. R.; Oseroff, A. R.; Dougherty, T. J.; Pandey, R. K. Synthesis of beta-galactose-conjugated chlorins derived by enyne metathesis as galectin-specific photosensitizers for photodynamic therapy. *J. Org. Chem.* **2001**, *66*, 8709–8716.

**Chart 1.** Photosensitizers Related to Pyropheophorbide-a

Structures Related to Pyropheophorbide-a (PPA)	R1 Substituent	Position of R1	Linkage	Relative Change	#
<b>Pyropheophorbide-a</b>					
	-CH(CH <sub>3</sub> )	3		2.82	<b>1<sup>a,b</sup></b>
	-CH(O-hexyl)CH <sub>3</sub>	3	Ether	2.99	<b>2<sup>a,b</sup></b>
	-CH(O-decyl)CH <sub>3</sub>	3	Ether	1.42	<b>3<sup>b</sup></b>
	-(iodobenzyloxy)CH <sub>3</sub>	3	Ether	2.5	<b>4<sup>a,c</sup></b>
<b>3-(iodobenzyloxy)CH<sub>3</sub> PPA</b>					
	-Galactose	17	Amide (Flexible)	0.97	<b>5<sup>d</sup></b>
	-Glucose	17	Amide (Flexible)	1.15	<b>6<sup>d</sup></b>

<sup>a</sup>Compounds **1** and **2** are commonly known as pyropheophorbide-a (PPA) and HPPH respectively. Compound **4** is 3-(1'-*m*-iodobenzyloxy) pyropheophorbide-a.

<sup>b</sup>Reference 33.

<sup>c</sup>Reference 1.

<sup>d</sup>Reference 5.

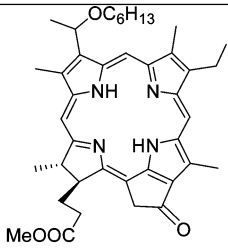
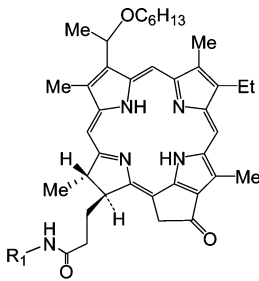
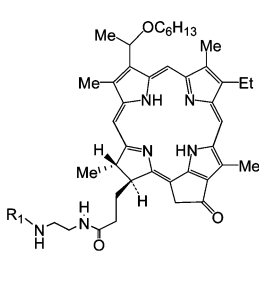
**Assessment of Side Population before and after *in Vitro* PDT.** The SP in 4T1 tumor cells was determined by flow cytometry on an LSR II flow cytometer using Dye Cycle Violet, a cell permeable violet laser (405 nm) excited alternative to the UV excited Hoechst 33342, with similar properties for determination of SP.<sup>44,45</sup> 4T1 tumor cells were seeded at 10<sup>6</sup> in 10 mL of growth medium in replicate 100 mm tissue culture plates, cultured for 48 h and then incubated for 4 h with 800 nM HPPH (**2**) or HPPH-Gal (**8**) (ABCG2 substrate and nonsubstrate PS, respectively) in the presence or absence of 10  $\mu$ M IM. Cells were irradiated with light (1 J/cm<sup>2</sup> at 3.2 mW/cm<sup>2</sup>) and further incubated for 48 h to allow targeted cells to die. These conditions caused an approximate cell kill of between 80 and 90%. Controls were untreated,

irradiated with light or incubated with PS in the dark or with 10  $\mu$ M IM in the dark or light. After 48 h the remaining cells were harvested, adjusted to 2  $\times$  10<sup>6</sup> cells mL<sup>-1</sup> and incubated for 90 min at 37 °C with DCV (10  $\mu$ M) with and without ABCG2 inhibitors (FTC or IM) in RPMI containing 2% FCS, centrifuged, and resuspended in cold RPMI containing 2% FCS and 2  $\mu$ g/mL 7-amino actinomycin D (7-AAD), a fluorescent live/dead discriminator taken up by dead cells. Samples were placed on ice, to prevent energy dependent efflux of DCV. The relative proportions of SP in the remaining live cells were determined immediately by flow cytometry by placement of a series of gates on dot plots as described.<sup>44,45</sup> Briefly, cells were gated on FSC and SSC, a live gate was placed on cells excluding 7-AAD (Ex 488 nm, Em 685/35 nm) and single cells were gated based on the 405 nm excited blue fluorescence cell cycle (450/50 nm area vs width). The SP was determined by a gate placed on the 405 nm excited blue (450/50 nm) vs red (645 nm long-pass) fluorescence dot plot. The gate was placed below the fluorescence observed by using the specific inhibitors FTC

(44) Telford, W. G.; Bradford, J.; Godfrey, W.; Robey, R. W.; Bates, S. E. Side population analysis using a violet-excited cell-permeable DNA binding dye. *Stem Cells* **2007**, 25, 1029–1036.

(45) Mathew, G.; Timm, E. A., Jr.; Sotomayor, P.; Godoy, A.; Montecinos, V. P.; Smith, G. J.; Huss, W. J. ABCG2-mediated DyeCycle Violet efflux defined side population in benign and malignant prostate. *Cell Cycle* **2009**, 8, 1053–1061.

**Chart 2.** Carbohydrate Analogues of HPPH (2-(1'-Hexyloxyethyl) Pyropheophorbide-a) Linked at Position 17 with a Flexible Amide Bond or a Rigid Amino–Amide Linker

Structures Related to HPPH <sup>a</sup>	R1 Substituent	Position of R1	Linkage	Relative Change	#
<b>HPPH</b>					<b>2</b>
					
	-Lactose	17	Amide (Flexible)	0.98	<b>7</b>
	-Galactose	17	Amide (Flexible)	1.07	<b>8</b>
	-Cellobiose	17	Amide (Flexible)	1.1	<b>9</b>
	-Glucose	17	Amide (Flexible)	1.06	<b>10</b>
	-Peracetylated Galactose	17	Amide (Flexible)	1.03	<b>11</b>
	-Monolactose	17	Amino-amide (Rigid)	1.13	<b>12</b>
	-Dilactose	17	Amino-amide (Rigid)	1.04	<b>13</b>
	-Tetralactose	17	Amino-amide (Rigid)	1.03	<b>14</b>

<sup>a</sup>Reference 26.

or IM to inhibit efflux of DCV which causes the SP to disappear as the fluorescence increase shifts the population. Figure 7 illustrates the population shift.

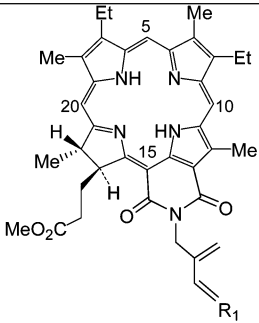
**In Vitro Phototoxicity of Substrate PS on Isolated SP and NON-SP 4T1 Cells.** SP and NON-SP were isolated from 4T1 cells by sorting on a FACSaria flow cytometer, based on DCV exclusion for the SP and retention for the NON-SP. Gates for delineation of the SP were set as described for the LSR II above. Isolated cells were seeded in 96-well plates at  $10^3$ /well. HPPH (200, 400, or 800 nM) was added, incubated for 4 h and then exposed to 1 J/cm<sup>2</sup>

of red light at 3.2 mW/cm<sup>2</sup>. The fraction of surviving cells was determined 48 h later by the colorimetric based MTT assay.

**The Effect of PDT on SP in 4T1 Tumors Grown *in Vivo*.** The experimental animal protocol was approved by the Institutional Animal Care and Use Committee (IACUC) at Roswell Park Cancer Institute. Female BALB/c mice 8–10 weeks old (Charles River, Wilmington, MA) with freely accessible standard mouse chow and water were inoculated subcutaneously on the shoulder with  $3 \times 10^5$  4T1 cells. Mice bearing 4T1 tumors (approximately 6 mm diameter, 6–7



**Chart 3.** Lactose Analogues of N-Substituted Mesopurpurinimide (**15**)

Structures related to Purpurinimides <sup>a</sup>	R1	Substituent position	Linkage	Relative Change	#
N-substituted meso-purpurinimides					
	-H	13 <sub>2</sub>	Diene	1.84	<b>15</b>
	-Lactose	13 <sub>2</sub>	Alkoxydiene	1.07	<b>16</b>
	-Lactose	13 <sub>2</sub>	Aryl-acetylene-ether	0.92	<b>17</b>

<sup>a</sup>References 36 and 43.

days after inoculation of tumor cells) were administered 0.47  $\mu\text{mol/kg}$  HPPH or HPPH-Gal *via* tail vein injection followed 24 h later by 135 J/cm<sup>2</sup> at 75 mW/cm<sup>2</sup> red laser light (665 nm) to the tumor (standard PDT dose). Tumors were harvested 48 h later and disaggregated by mincing finely and incubating at 37 °C with gentle mixing in HBSS containing 0.25% collagenase, 0.25% protease Type IX (Sigma) and 0.02% DNase I (U.S. Biochemical) to release the cells. Cells were washed and filtered to remove aggregates, adjusted to  $2 \times 10^6$  mL<sup>-1</sup>, and then incubated in medium containing 2% FCS and 10  $\mu\text{M}$  DCV, with and without ABCG2 inhibitors and 7-AAD. The proportion of SP in remaining live cells was determined by flow cytometry.

#### Detection of ABCG2 Activity on Various Cell Lines.

To determine whether there was functional ABCG2 activity in a selection of tumor cell lines, cells were incubated with HPPH with or without IM as described above for HEK-293 cells and fluorescence was measured by flow cytometry. The presence and size of SP levels in the tumor cell lines was determined by incubation with DCV with or without IM or FTC as described for 4T1 cells.

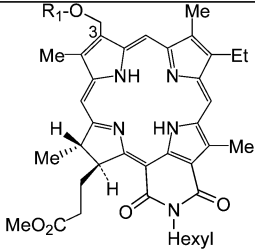
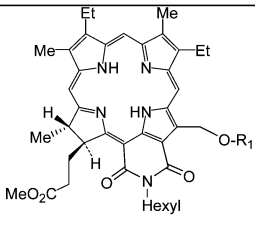
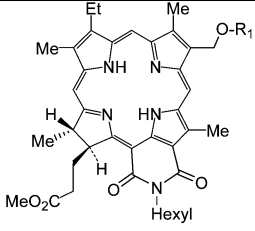
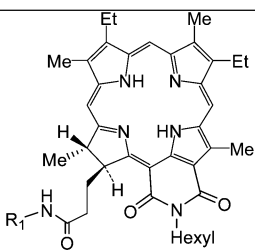
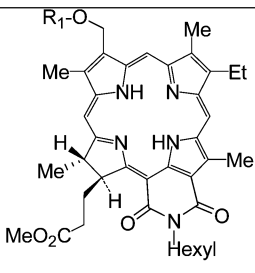
**Immunohistological Detection of ABCG2.** To examine the cellular distribution of ABCG2 in cells which were functionally responsive or nonresponsive to its inhibition by IM by flow cytometry with HPPH, cells were stained with

antibody to (human) ABCG2. Harvested cells (of human origin) were pelleted, fixed in 10% neutral formalin and embedded in paraffin. Reagents were from DakoCytomation, Carpinteria, CA, unless otherwise indicated. Sections were processed by standard methods and stained for ABCG2 expression with BXP-21 antibody (Alexis Biochemicals) based on Diestra et al.<sup>46</sup> Immune reactions were detected with the Envision+ Dual Link System-HRP kit. Briefly, antigen retrieval (20 min in a steamer) was performed with citrate buffer pH 6.0 (Biogenex, San Ramon, CA), and then blocking and washing was performed according to the kit instructions. After blocking, sections were incubated at 4 °C overnight with 1/50 BXP-21 (5  $\mu\text{g/mL}$ ) or an equivalent concentration of isotype control IgG2a diluted in Antibody Diluent. Staining was completed according to the kit instructions using DAB+ as chromogen, counterstained with hematoxylin (Richard Allen Scientific, Kalamazoo, MI) and mounted for microscopic examination.

- (46) Diestra, J. E.; Scheffer, G. L.; Catala, I.; Maliepaard, M.; Schellens, J. H.; Scheper, R. J.; Germa-Lluch, J. R.; Izquierdo, M. A. Frequent expression of the multi-drug resistance-associated protein BCRP/MXR/ABCP/ABCG2 in human tumours detected by the BXP-21 monoclonal antibody in paraffin-embedded material. *J. Pathol.* **2002**, *198*, 213–219.



**Chart 4.** Carbohydrate Analogues of *N*-Hexyl-purpurinimide (**18**) and 3-Hydroxymethyl-*N*-Hexyl-purpurinimide (**22**)

Structures related to <i>N</i> -hexyl-purpurinimides <sup>a</sup>	R1	Substituent position	Linkage	Relative Change	#
	-Lactose	3	Ether	1.00	<b>18</b>
	-Lactose	12	Ether	1.03	<b>19</b>
	-Lactose	8	Ether	1.12	<b>20</b>
	-Lactose	17	Amide	0.94	<b>21</b>
	-H	3	Ether	1.65	<b>22</b>
	-Glucose	3	Ether	1.72	<b>23</b>
	-Galactose	3	Ether	1.89	<b>24</b>

<sup>a</sup>Reference 36.

## Results

We previously found that conjugating a  $\beta$ -galactoside carbohydrate (galactose) and other carbohydrates at position 17 of the macrocycle of HPPH inhibited efflux by ABCG2.<sup>12,26</sup>

Our goal was to determine if substitutions in other compounds and in other positions also could affect interactions of the photosensitizer with ABCG2. The photosensitizers tested were pyropheophorbides and purpurinimides (see

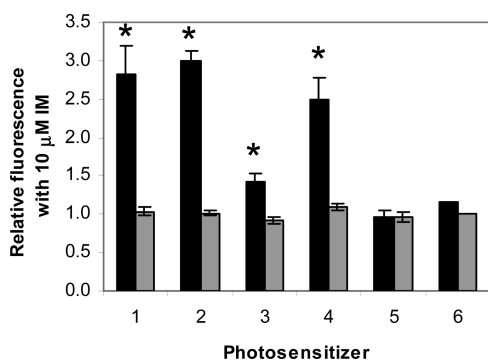


**Figure 1.** The effect mediated by the TKI IM on fluorescence produced by photosensitizers related to pyropheophorbide-a (PhA) with different groups attached to the macrocycle, as indicated in Chart 1. Bars are mean  $\pm$  SEM of 2–13 experiments with triplicate samples for each compound. HEK 293 482R cells (ABCG2+) (black bars), HEK 293 PcDNA cells (ABCG2–) (gray bars). \* $P$  < 0.05.

Charts 1–4) to which different peripheral groups were attached for analyzing phototoxicity efficacy in SAR studies, and their synthesis has mostly been published elsewhere.<sup>1,2,8,26,36,43</sup> The substituents included molecules such as iodobenzene that facilitate the use of the PS as potential PET contrast agents,<sup>2,4,5</sup> or that alter the lipophilicity of the PS such as alkyl groups.<sup>8</sup> A variety of mono- and disaccharide groups, namely, the  $\beta$ -galactosides galactose and lactose, and non  $\beta$ -galactosides glucose and cellobiose attached with different linking moieties (ether, diene, acetylene or amide) to the same or different positions on the photosensitizers, also were investigated.<sup>1,4,5,26,36</sup> We also examined effects of the mono-, di-, and tetrameric disaccharide lactose conjugated to HPPH by a rigid (amino–amide) linker.<sup>26</sup> In other compounds the position (3, 8, 12, 13, 17, 13<sub>2</sub>) at which the lactose was conjugated to the macrocycle was varied.<sup>26,36</sup>

**Flow Cytometry Analysis of Affinity of Photosensitizers for ABCG2.** The fluorescence change mediated by the TKI IM in the two cell lines HEK-293 PcDNA (ABCG2 negative) and HEK-293 428R (ABCG2 positive) is expressed as the (fractional) change relative to the fluorescence due to the PS alone. In HEK-293 PcDNA cells incubated with PS in the presence of IM, no significant change in fluorescence was observed in all cases. Increased fluorescence mediated by IM for some of the PS was observed in HEK-293 428R, indicating they were substrates for ABCG2. The numerical values for the relative changes are shown in Charts 1–4.

Similar to the report by Robey for PhA<sup>18</sup> we found that PPA (**1**) is strongly effluxed by ABCG2 as indicated by the increase in fluorescence (1.8) mediated by IM in HEK-293 482R ABCG2+ cells (Figure 1). The affinity of substituted analogues is defined relative to the change observed in PPA fluorescence due to IM. Addition of a 6-carbon alkyl chain (**2**, HPPH) with an ether linkage at position 3 of PPA had little effect on its affinity, being strongly effluxed as indicated by a similar increase in fluorescence mediated by IM (2.0), but a 12-carbon chain (**3**) decreased efflux markedly (the increase in fluorescence due to IM being only 0.42). Addition

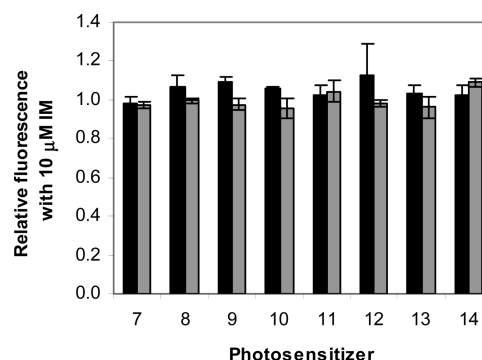


**Figure 2.** Carbohydrate substitutions on HPPH. The effect mediated by the TKI IM on fluorescence produced by HPPH with different groups attached to the macrocycle, as indicated in Chart 2. Bars are mean  $\pm$  SEM of 2–3 experiments with triplicate samples for each compound. HEK-293 482R cells (black bars), HEK-293 PcDNA cells (gray bars).

of iodobenzene at position 3 (**4**) decreased affinity slightly (1.5 increase in fluorescence). Conjugation of galactose (**5**) or glucose (**6**) at position 17 with an amide linkage completely changed the affinity of iodobenzyl-PPA for ABCG2 in HEK-293 482R cells, with no changes in fluorescence observed in the presence of IM. As expected, no fluorescence differences were observed with any of the compounds when incubated with the ABCG2– HEK-293 PcDNA cells. Also as expected, because of its lower ABCG2 expression, RIF cells exhibited similar, but considerably less pronounced, changes under these conditions, which depended somewhat on the PS (Figures 2–4 in the Supporting Information).

Since monosaccharides added at position 17 on PPA abrogated its affinity for ABCG2, we examined the effect of different carbohydrates added at position 17 on HPPH, another strongly ABCG2-effluxed compound (Chart 2).

Not only did addition of the monosaccharides galactose **8** and glucose **10** to HPPH with an amide linkage prevent efflux of these compounds but so also did addition of the disaccharides lactose **7** and cellobiose **9** (Figure 2). Thus, the orientation of the OH bonds on the disaccharides did not influence affinity for ABCG2, as previously found for galactose and glucose conjugates. Indeed, in the absence of the OH bonds in either orientation **11** (peracetylated form) there still was no drug efflux mediated by ABCG2, suggesting that the effect, at least at position 17, is not restricted to carbohydrates. Changing the conjugation to HPPH of lactose **12** and multimers of lactose **13** and **14** (dilactose and tetralactose) to a rigid linker (amino–amide) had a similar effect on affinity, with no significant efflux of these compounds (Figure 2).

To determine whether the observations with PPA and HPPH extended to other chlorins, we examined the effect on ABCG2 substrate affinity of linking lactose to various positions on the purpurinimide macrocycle, and also with different linkers to see if this was a structural effect confined to position 17. The compounds are shown in Charts 3 and

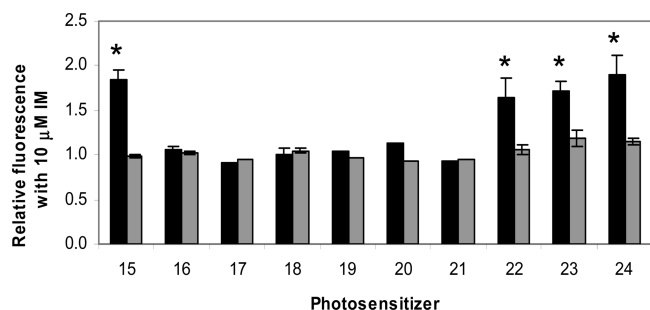


**Figure 3.** The effect mediated by the TKI IM on fluorescence produced by purpurinimides (**15** and **22**) with lactose attached at different positions of the macrocycle (**16–21**), and glucose (**23**) or galactose (**24**) attached at position 3 as indicated in Charts 3 and 4. Bars are mean  $\pm$  SEM of 2–5 experiments with triplicate samples for each compound. HEK-293 482R cells (black bars), HEK-293 PcDNA cells (gray bars). \* $P < 0.05$ .

4. Figure 3 shows that the unsubstituted purpurinimide(s) **15** and **22** also were substrates of ABCG2, albeit of lesser affinity than the pyropheophorbide-based compounds, with smaller increases in fluorescence of 0.84 and 0.65 respectively mediated by the inhibitor IM. However, as with the pyropheophorbides, substitution of lactose at position 17 (**21**) produced a nonsubstrate, as did lactose at positions 8 (**20**), 12 (**19**) and 13<sub>2</sub> (**17**) (Figure 3). Substitution of galactose (**24**) or glucose (**23**) at position 3 on the purpurinimide did not decrease its affinity, with fluorescence increases of 0.89 and 0.72 respectively (Figure 3), in common with the various substitutions at the same position in PPA. In contrast, lactose at position 3 (**18**) produced a nonsubstrate (Figure 3).

Changing the linker did not appear to influence changes in affinity, at different positions, or with different substituents. Thus lactose attached with an ether (**18**, **19**, **20**, **21**), a diene (**16**), an acetylene (**17**) an amide (**7**) or an amino–amide (**12**) linker at all positions tested abrogated transport by

ABCG2. However, an ether linkage could be attached to substituents that maintained, hexyl (**2**) and iodobenzene (**4**); decreased, decyl (**3**); or eliminated substrate transport, lactose (**18**). Not all possible combinations and positions have been tested, but thus far the most variable influence appears to be at position 3 where the characteristics of the substituents appear to be the most important criteria for conferring affinity or eliminating transport.

**Side Population Analysis of 4T1 Cells.** A prominent FTC and IM inhibitable SP was found in 4T1 cells (Figure 4) which ranged from 4 to 15% of the total population *in vitro* (shown as the mean in Figure 5A), and 2 to 20% *in vivo* (shown as the mean in Figure 6). The example in Figure 4 shows a SP of 5.6% in 4T1 cells grown *in vitro*. The *in vivo* tumor samples were not labeled to differentiate lineage positive cells, so the SP will contain any ABCG2 positive stromal or infiltrating cells as well as tumor SP. This may inflate the size of the SP *in vivo* somewhat compared with that seen in tumor cells cultured *in vitro*. However, regardless of source, ABCG2-expressing cells may pump out substrates.

**In Vitro PDT of Cells.** Treatment of 4T1 cells grown *in vitro* with PDT using substrate HPPH and nonsubstrate HPPH-Gal caused an increase of the proportion of SP in surviving cells with HPPH and a decrease of the SP with HPPH-Gal (Figure 5A). This suggested that the SP in HPPH incubated cells were less susceptible to PDT than those incubated with HPPH-Gal. When IM was present during incubation of 4T1 cells with the PS, subsequent light irradiation decreased the SP of the HPPH incubated cells, suggesting that it was responsible for retention of the HPPH in the cells and the better PDT response (Figure 5A).

**In Vitro PDT of SP, NON-SP, and Unsorted 4T1 Cells.** To confirm that the SP cells were resistant to HPPH we performed PDT on unsorted and sorted SP and NON-SP cells. Figure 5B clearly shows that the sorted SP cells are resistant to HPPH-PDT compared to unsorted and NON-SP 4T1 cells. The curve obtained from mathematically com-

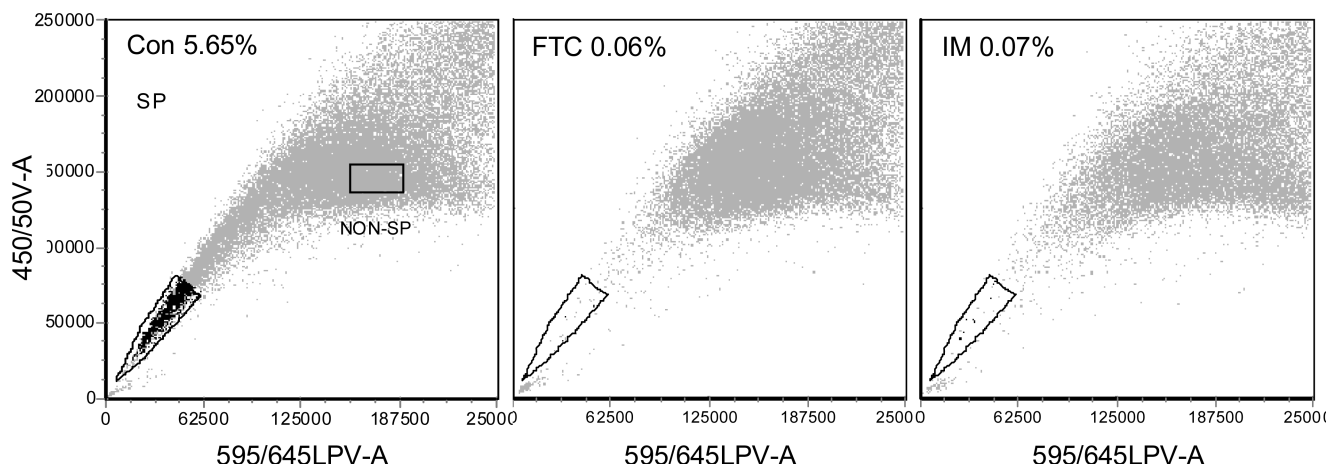


**Figure 4.** Flow cytometry dot plots with red fluorescence on the x-axis and blue fluorescence on the y axis, showing the side population (SP) in 4T1 cells grown *in vitro* and stained with DCV. The numbers in the plots show the SP as a percentage of the single live cells in the gated population, with DCV alone, control, left: Con, or incubated with the inhibitors FTC and IM. The SP and NON-SP gates in the control show the population from which cells were sorted for comparative phototoxicity with HPPH-PDT.

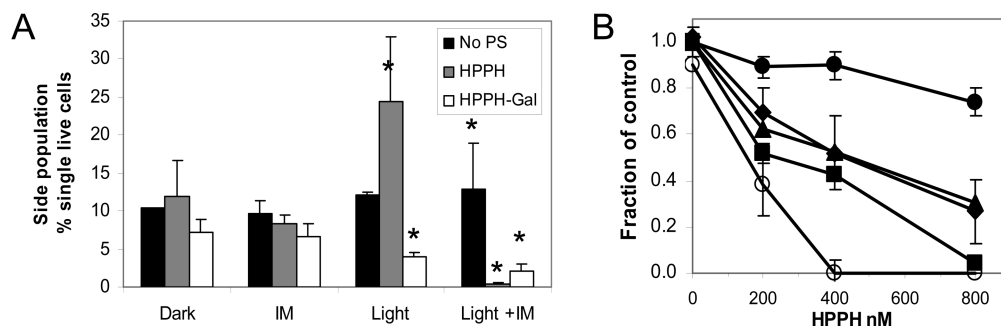


**Figure 5.** A: The SP remaining in 4T1 cells treated *in vitro* with HPPH or HPPH-Gal PDT in the presence and absence of IM. Cells were incubated for 4 h with 800 nM HPPH or HPPH-Gal, in the presence or absence of 10  $\mu$ M IM and irradiated with 1 J/cm<sup>2</sup> then harvested and stained with DCV 48 h later. Bars are mean and SD of 3 experiments. \*Significantly different from dark groups  $P < 0.05$ . B: Dose response curves of HPPH-PDT of sorted SP and NON-SP (from populations indicated in Figure 4) and unsorted 4T1 cells treated *in vitro* with HPPH PDT. Cells were incubated for 4 h with HPPH and irradiated with 1 J/cm<sup>2</sup>, and then the surviving fraction was determined by the colorimetric MTT assay 48 h later. Mean and SD of 3 experiments: sorted SP (●); sorted SP + IM (○); sorted NON-SP (■); unsorted cells (◆); combined phototoxicity data from sorted SP and NON-SP (▲), determined by mathematical combination of sorted SP and NON-SP surviving fractions: [1 – (non surviving fraction NON-SP – non surviving fraction SP)].

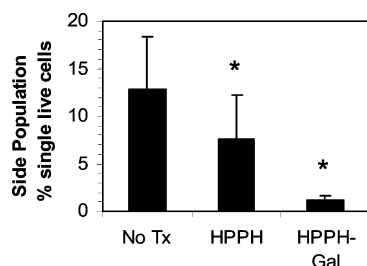


**Figure 6.** The SP in cells from 4T1 tumors treated *in vivo* with HPPH or HPPH-Gal PDT (0.47  $\mu$ mol/kg iv and irradiated 24 h later with 665 nm laser light, 135 J/cm<sup>2</sup> at 75 mW/cm<sup>2</sup>). Tumors were harvested 48 h later, disaggregated and stained with DCV and 7-AAD to determine the SP of surviving cells by flow cytometry. Bars are the accumulated means and SD of 4–5 samples from 2 experiments containing 1–3 pooled tumors in each sample. \*Significantly different from untreated group,  $P < 0.05$ . Tumors were pooled to obtain sufficient cells for a statistically valid analysis, since some of the tumors were very responsive to treatment, and few cells were recovered.

binning the phototoxicity of sorted SP and NON-SP data overlapped that obtained experimentally for the unsorted cells. As with the unsorted PDT cells in Figure 5A, addition of IM during incubation of sorted SP cells with HPPH enhanced phototoxicity, counteracting the resistance to PDT.

**In Vivo PDT of Tumors: Effect on SP.** To determine whether the resistance of SP to HPPH-PDT observed *in vitro* held also *in vivo*, 4T1 tumors were treated with PDT using HPPH or HPPH-Gal, and the proportion of SP in surviving cells isolated from disaggregated tumors 48 h later was determined.

Tumors treated with HPPH-PDT had a significantly higher proportion of residual SP than those treated with HPPH-Gal PDT (Figure 6), confirming that the relative resistance

observed with HPPH-PDT SP *in vitro* (Figure 5) also occurs *in vivo*. The SP from PDT with HPPH was lower than that found in untreated tumors, implying that at the dose used some targeting of the SP by HPPH occurs and indicating that sufficient HPPH was retained to reach the threshold for phototoxicity in some SP cells.

**Enhancement of HPPH Retention and Presence of SP in Several Cell Lines.** Several additional cell lines often used in experimental PDT were incubated with HPPH as substrate with and without IM to determine whether functional ABCG2 was present and to examine its effect on HPPH retention. Some of the cell lines, A549, RIF, Colon26A and HeLa+, had significantly increased HPPH fluorescence in the presence of IM over HPPH alone (Figure 7A). Those cells in Figure 7A without significant enhancement of HPPH with IM, namely, HeLa–, FaDu, U87 and Colon26B, were additionally tested for the presence and size of a SP after incubating with DCV. In all of these cell lines a SP with DCV (inhibitable with IM or FTC) was found (Figure 7B), indicative of the presence of ABCG2 in this small population. This suggests that those cells in the side population might also be resistant to HPPH PDT as was found for the SP in 4T1 cells and tumors. Resistance of the SP in U87 to the ABCG2 substrate PpIX (synthesized endogenously from exogenously administered aminolevulinic acid, ALA) was previously found *in vitro*.<sup>13</sup>

**Cellular ABCG2 Distribution by Immunostaining.** As expected, staining cells for ABCG2 showed strong immunopositivity in HEK-293 482R cells with a prominent cell membrane distribution (Figure 8A). HEK-293 PcDNA cells were negative for ABCG2 (Figure 8B) as were FaDu (Figure 8E) and U87 (Figure 8F), consistent with the absence of a change in HPPH fluorescence in response to IM. Of note, the two different sources of HeLa cells which showed differential ABCG2 activity were positive (Figure 8C) and



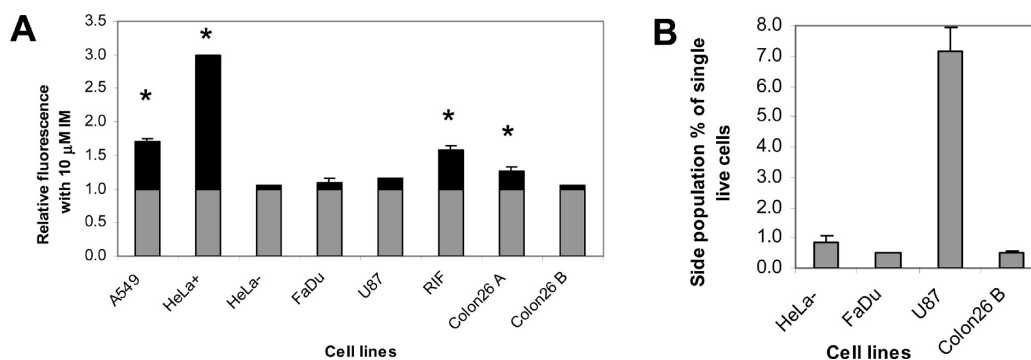


**Figure 7.** A: Relative change in HPPH fluorescence of several cell lines after incubation in the absence and presence of 10  $\mu$ M IM. The black portion of the columns indicates the relative change above the level of fluorescence found by incubating with HPPH alone. \* indicates a significant change in HPPH fluorescence mediated by IM ( $p < 0.05$ ). B: SP present in cell lines in which the relative change in HPPH fluorescence after incubation in the presence of 10  $\mu$ M IM was not significantly different from incubation with HPPH alone.

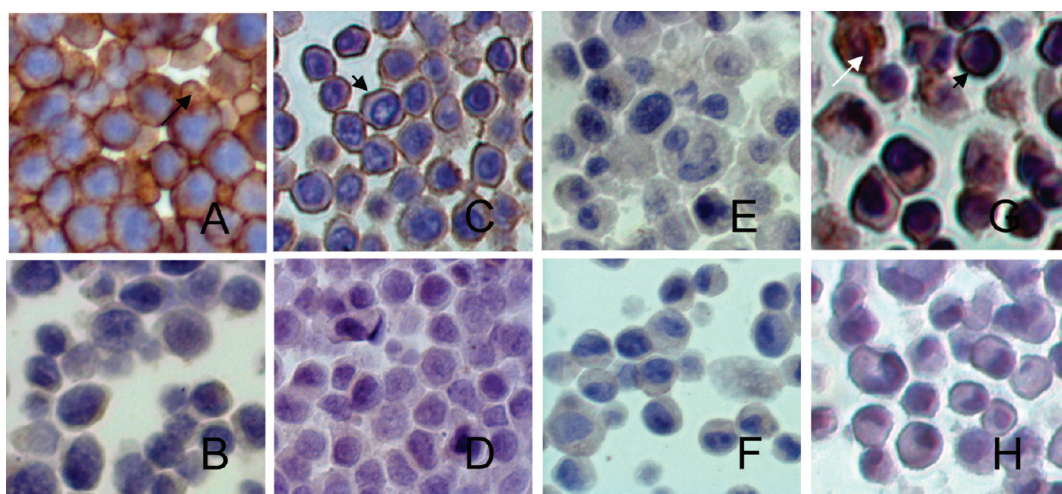


**Figure 8.** ABCG2 distribution after immunostaining with BXP-21 antibody to human ABCG2. A: HEK-293 R482A. B: HEK-293 PcDNA. C: HeLa (ABCG2+). D: HeLa (ABCG2-). E: U87. F: FaDu. G: A549. H: A549 (isotype control). Short arrows: membrane ABCG2. Long arrow: cytoplasmic ABCG2. White arrow: nuclear ABCG2.

negative (Figure 8D) for immunoreactive ABCG2, with a primarily membrane localization indicative of functional ABCG2 in the HeLa+ cells. A549 was positive for ABCG2 (Figure 8G) with a membrane distribution in some cells and cytoplasmic or nuclear staining in others. The isotype controls (shown for A549) were negative for ABCG2 (Figure 8H). The amount of cell membrane ABCG2 staining correlates qualitatively with the degree of functional ABCG2 activity demonstrated by HPPH retention in the cells as shown in Figure 7A. Only human cells were reactive with the BXP-21 antibody for immunohistochemistry, so the murine tumor cells were not stained.

## Discussion

We have shown here that certain PS are substrates of the ABCG2 transporter and that ABCG2 is expressed at different levels on cell lines used in many *in vitro* and *in vivo* tumor models for PDT which may affect phototoxic efficacy. ABCG2 expression and function at relatively high levels was represented here by RIF, lung cancer A549 and cervical cancer HeLa+; at lower levels on colon carcinoma Colon26A;

and in the SP (determined by DCV staining) of other cell lines some of which appeared to be ABCG2 negative by immunostaining or Western blot.<sup>12</sup> the murine tumors 4T1 and Colon26B and the human tumor cell lines FaDu, U87 and HeLa-. Some of the compounds tested here were demonstrated previously to be an ABCG2 substrate (e.g., HPPH) or a nonsubstrate (e.g., HPPH-Gal).<sup>12</sup> Their use in this study confirms their affinity, and further allows their use as internal controls for the flow cytometry assay.

Certain criteria were important for ABCG2 substrate affinity. (1) The unsubstituted pyropheophorbides and purpurinimides were all ABCG2 substrates. (2) The conjugation of carbohydrates to the macrocycle at positions 8, 12, 13, and 17 abrogated affinity for ABCG2. This occurred regardless of the nature of the linking agents, or the type of attached carbohydrates (mono- and disaccharides or multimers). This is not exclusively a carbohydrate feature since we have also found similar effects for non-carbohydrate compounds at position 17 in pyropheophorbides (not shown). (3) For substitutions at position 3, ABCG2 substrate affinity depended somewhat on the nature of the group added. Addition

of iodobenzene (**4**) or a hexyl group to pyropheophorbide (**2**) *via* an ether linkage did not affect affinity whereas the longer decyl carbon chain (**3**) decreased efflux somewhat. Similarly, the monosaccharides glucose and galactose at position 3 in a purpurinimide, compounds **23** and **24** respectively, did not affect ABCG2 affinity, both being effluxed; but attachment of the disaccharide lactose at position 3, compound **18**, produced a nonsubstrate. Possibly the larger sizes of the C12 and the lactose (compared to the hexyl and monosaccharides) interfered with access to the binding domain of ABCG2. The implications here are that the compounds have structural features at and around position 3 of the macrocycle that are important for binding to and efflux by ABCG2, barring other substitutions at other positions that also could affect binding.

The flow cytometry assay used here to determine PS substrate specificity and affinity for ABCG2 is simple, and easily adaptable depending on the resources available. Most standard flow cytometers have adequate excitation sources at 488 nm 633 and 405 nm and detection channels to measure fluorescence emission from photosensitizers. Our standard conditions were 1  $\mu$ M PS, incubated for 90 min at 37 °C in medium containing 2% serum after preincubation with the inhibitors, which proved adequate for most of the PS used here. However, detailed kinetics, and alternative assay conditions and PS or serum concentrations to prevent saturation of the pump, may be required to fully dissect the affinity of the PS for the transporter. At the standard concentration some PS (due to their physicochemical characteristics) may be aggregated. Compound **3** with a 12-carbon alkyl ether group at position 17 is somewhat aggregated at this concentration and may be too bulky to access the binding site on ABCG2, which could account for its diminished efflux compared to HPPH, which has a shorter hexyl chain (Chart 1). Exogenous PpIX (again highly aggregated at 1  $\mu$ M) also was a poor substrate under these conditions (not shown), although it is strongly effluxed when synthesized endogenously from ALA in ABCG2-expressing cells.<sup>12,13</sup>

The HEK-293 cells maintained in a selection medium demonstrate extremely stable and reproducible ABCG2 expression and function, but almost any cell line expressing sufficient functional ABCG2 in the cell membrane can be used to test PS affinity for the pump, for example A549 has been shown to express high ABCG2.<sup>40</sup> We showed in Figure 7 that A549 and a variety of cells used as tumor models for determining phototoxic efficacy have enhanced HPPH retention when ABCG2 is inhibited by IM. We used HPPH as the fluorescent substrate to demonstrate ABCG2 activity since it is used increasingly in clinical studies and has become the standard against which we test the potential of many newly synthesized photosensitizers. As a note of caution, the ABCG2 expression status of many cell lines may fluctuate related to the confluency or density of the cell

cultures.<sup>12,13,46–50</sup> Fluctuations in the size of the SP also may depend on the contribution of ABCG2-expressing cells to the proliferation potential of the cell line.<sup>29,48,50</sup> When testing for ABCG2 substrate specificity and affinity with undefined cell lines, it is important to monitor the consistency of performance of the assay by including known substrates such as PhA (Frontier Scientific, Logan, UT) or HPPH.

Although it was not examined here in any detail since it has been published elsewhere, nonsubstrates might be expected to have better phototoxicity than substrates in ABCG2-expressing cells, since they are retained in cells instead of being transported out. However, other factors may influence uptake, retention and phototoxicity, such as lipophilicity and localization. For example *in vitro* in the purpurinimide series, despite being substrates, compounds **23** and **24** with glucose and galactose substitutions had higher uptake/retention and better phototoxicity than the unsubstituted substrate precursor **22**.<sup>36</sup> Further, cellular levels of **23** and **24** were considerably higher than the nonsubstrate **18** substituted with lactose, but phototoxicity was less marked, suggesting that it is not cellular concentrations alone which define the PDT response.<sup>36</sup> Compounds **23** and **24** were localized to lysosomes, whereas **18** had a mixed lysosomal/Golgi apparatus distribution, and **22**, the least effective PS at the lowest cellular levels, was primarily found in the Golgi apparatus, so localization may play a role.<sup>36</sup> In contrast, compound **3**, a lipophilic substrate, albeit with lower transport than the less lipophilic HPPH, is localized primarily in lysosomes at the incubation concentrations used here, whereas HPPH is found primarily in mitochondria.<sup>51</sup> The position 17 mono- and disaccharide analogues of HPPH, all nonsubstrates, are all hydrophilic, with primarily lysosomal localization.<sup>26</sup> The ABCG2 substrate mitoxantrone also has a primarily lysosomal localization, and we have tested other compounds with a mitochondrial localization which are nonsubstrates (unpublished observations). Thus, no clear

- 
- (47) Loebinger, M. R.; Giangreco, A.; Groot, K. R.; Prichard, L.; Allen, K.; Simpson, C.; Bazley, L.; Navani, N.; Tibrewal, S.; Davies, D.; Janes, S. M. Squamous cell cancers contain a side population of stem-like cells that are made chemosensitive by ABC transporter blockade. *Br. J. Cancer* **2008**, *98*, 380–387.
- (48) Mitsutake, N.; Iwao, A.; Nagai, K.; Namba, H.; Ohtsuru, A.; Saenko, V.; Yamashita, S. Characterization of side population in thyroid cancer cell lines: cancer stem-like cells are enriched partly but not exclusively. *Endocrinology* **2007**, *148*, 1797–1803.
- (49) Platet, N.; Mayol, J. F.; Berger, F.; Herodin, F.; Wion, D. Fluctuation of the SP/non-SP phenotype in the C6 glioma cell line. *FEBS Lett.* **2007**, *581*, 1435–1440.
- (50) Tavaluc, R. T.; Hart, L. S.; Dicker, D. T.; El Deiry, W. S. Effects of low confluency, serum starvation and hypoxia on the side population of cancer cell lines. *Cell Cycle* **2007**, *6*, 2554–2562.
- (51) MacDonald, I. J.; Morgan, J.; Bellnier, D. A.; Paszkiewicz, G. M.; Whitaker, J. E.; Litchfield, D. J.; Dougherty, T. J. Subcellular localization patterns and their relationship to photodynamic activity of pyropheophorbide-a derivatives. *Photochem. Photobiol.* **1999**, *70*, 789–797.
- (52) Yanase, K.; Tsukahara, S.; Asada, S.; Ishikawa, E.; Imai, Y.; Sugimoto, Y. Gefitinib reverses breast cancer resistance protein-mediated drug resistance. *Mol. Cancer Ther.* **2004**, *3*, 1119–1125.

pattern of localization, cellular levels or lipophilicity explains affinity for the ABCG2 transporter and the phototoxic response completely, but it is clear that ABCG2 levels can influence the comparative response by altering levels of substrate PS. It is possible that some of the PS may not be transported by ABCG2 because their uptake mechanism evades exposure to the transporter, rather than the structural considerations conferred by the added constituents, or *vice versa*. Of the purpurinimide series, only compound **18**, the nonsubstrate was an effective PDT agent *in vivo*, whereas the substrates **22**, **23** and **24** were ineffective at producing cures with PDT in the RIF tumor model which expresses ABCG2.<sup>36</sup> Similarly, *in vivo* with the pyropheophorbides, the nonsubstrate HPPH-galactose (**8**) was more effective in the RIF tumor model than the substrate HPPH (**3**).<sup>12,26</sup> In the same study the nonsubstrate **8** also was more effective *in vivo* than HPPH in the Colon26B model, which expresses ABCG2 only on the small (less than 1%) SP (Figure 7B). It is not known if the SP in Colon26 tumors is the true TIC in this model, but if it is, the use of the nonsubstrate PS **8** in preference to the substrate HPPH may have been responsible for the enhanced response.

We showed the importance of functional ABCG2 expression on a small population of cells to the PDT response with a substrate by isolating the SP from 4T1 cells and treating them with PDT with a substrate PS. Commonly used phototoxicity assays such as the MTT assay may not discriminate between different expression levels of ABCG2 within a heterogeneous population, especially if the population is very small, for example as in the SP of FaDu. As shown in Figure 5B, unsorted 4T1 cells appeared to respond well to PDT with HPPH. However, when the cells were separated into SP and NON-SP, their differential response to PDT in cells with ABCG2 activity became obvious, and resistance by SP cells could be overcome with an ABCG2 inhibitor. Similarly, colony forming assays (often used for testing cell viability after PDT) unless prolonged do not necessarily distinguish between SP and NON-SP responses, since both cell types may be capable of dividing the limited number of times required for scoring a colony of 50+ cells, typically achieved over 7–10 days.

To demonstrate the possible consequences of using ABCG2 substrate photosensitizers *in vivo* in the 4T1 murine mammary tumor model as a substitute for a clinical situation, we measured the relative proportion of surviving SP after PDT to show for the first time that ABCG2-expressing cells with potential tumor initiating capacity were relatively resistant to PDT with a substrate (HPPH) compared to a nonsubstrate (**8**) PS. The PDT conditions were not optimized for cures in these experiments, since sufficient surviving cells were required for measurements as proof of principal, but we have been able to achieve cures with substrate PS in animal tumor models expressing either high or low levels of ABCG2 or a SP, without compromising PDT specificity with overly high PS levels. However, in a clinical situation, conditions are more difficult to optimize than in reproducible animal models

and the reasons for partial responses or recurrences may be unclear. There is a strong possibility that PDT using substrate PS may result in the selective survival of ABCG2 positive cells which cause a recurrence in the same way that certain types of chemotherapeutic drugs may select for ABCG2-expressing cells in tumors which become resistant to subsequent therapy,<sup>52–54</sup> or upregulate ABCG2 expression and thus resistance by epigenetic changes.<sup>55</sup>

Cancer stem cells like normal stem cells are thought to be somewhat resistant to hypoxic conditions and prefer a hypoxic niche, which favors their maintenance and survival. Increased stresses such as hypoxia may encourage the proliferation of the SP<sup>50</sup> and homing of cancer stem cells toward hypoxic areas.<sup>56</sup> PDT itself may induce some degree of hypoxia by consumption of oxygen during the activation process, conferring another potential disadvantage for treatment of tumors with PDT using ABCG2 substrate PS. Adequate levels of PS and oxygen are required for a response. If ABCG2-expressing cells have pumped out substrate PS leaving levels too low for a phototoxic response, they have a double survival advantage, both to PDT itself and to the hypoxic environment induced by PDT that may promote their proliferation and regenerate the tumor. This characteristic of cancer stem cells reiterates the importance of a treatment regimen that maintains oxygen perfusion during PDT.

In summary, it is important to verify ABCG2 expression in tumors when choosing the most appropriate PS for treatment, especially if the PS is a substrate and if the ABCG2 positive SP cells are part of the tumor initiating population. If the NON-SP or ABCG2 negative populations include TIC, then the substrate specificity and affinity of the PS may be less important, since it will not be pumped out. Alternative methods to ensure adequate PS levels in all tumor cells would be to combine a substrate PS with a nonsubstrate PS, with an ABCG2 inhibitor such as IM, or to downregulate ABCG2 levels with modulators of the pathways that regulate ABCG2 expression, local-

- (53) Huang, Y.; Sadee, W. Membrane transporters and channels in chemoresistance and -sensitivity of tumor cells. *Cancer Lett.* **2006**, *239*, 168–182.
- (54) Al-Hajj, M.; Becker, M. W.; Wicha, M.; Weissman, I.; Clarke, M. F. Therapeutic implications of cancer stem cells. *Curr. Opin. Genet. Dev.* **2004**, *14*, 43–47.
- (55) Calcagno, A. M.; Fostel, J. M.; To, K. K.; Salcido, C. D.; Martin, S. E.; Chewing, K. J.; Wu, C. P.; Varticovski, L.; Bates, S. E.; Caplen, N. J.; Ambudkar, S. V. Single-step doxorubicin-selected cancer cells overexpress the ABCG2 drug transporter through epigenetic changes. *Br. J. Cancer* **2008**, *98*, 1515–1524.
- (56) Das, B.; Tsuchida, R.; Malkin, D.; Koren, G.; Baruchel, S.; Yeger, H. Hypoxia enhances tumor stemness by increasing the invasive and tumorigenic side population fraction. *Stem Cells* **2008**, *26*, 1818–1830.
- (57) Azzariti, A.; Porcelli, L.; Xu, J. M.; Simone, G. M.; Paradiso, A. Prolonged exposure of colon cancer cells to the epidermal growth factor receptor inhibitor gefitinib (Iressa(TM)) and to the antian-tiogenic agent ZD6474: Cytotoxic and biomolecular effects. *World J. Gastroenterol.* **2006**, *12*, 5140–5147.



ization and side population. Examples of the latter include IM, gefinitib (Iressa),<sup>57,58</sup> rapamycin,<sup>58</sup> and the PI3K inhibitor LY294402<sup>59</sup> which decreased the SP in U87 by 45–80%<sup>13</sup> and have been shown to regulate ABCG2 and/or SP localization or expression by translocation and/or posttranslational modifications of these and other signaling pathways.<sup>27,60,61</sup>

- (58) Elkind, N. B.; Szentpetery, Z.; Apati, A.; Ozvegy-Laczka, C.; Varady, G.; Ujhelly, O.; Szabo, K.; Homolya, L.; Varadi, A.; Buday, L.; Keri, G.; Nemet, K.; Sarkadi, B. Multidrug transporter ABCG2 prevents tumor cell death induced by the epidermal growth factor receptor inhibitor Iressa (ZD1839, Gefitinib). *Cancer Res.* **2005**, *65*, 1770–1777.
- (59) Zhou, J.; Wulfkühle, J.; Zhang, H.; Gu, P.; Yang, Y.; Deng, J.; Margolick, J. B.; Liotta, L. A.; Petricoin, E., III; Zhang, Y. Activation of the PTEN/mTOR/STAT3 pathway in breast cancer stem-like cells is required for viability and maintenance. *Proc. Natl. Acad. Sci. U.S.A.* **2007**, *104*, 16158–16163.
- (60) Takada, T.; Suzuki, H.; Gotoh, Y.; Sugiyama, Y. Regulation of the cell surface expression of human BCRP/ABCG2 by the phosphorylation state of Akt in polarized cells. *Drug Metab. Dispos.* **2005**, *33*, 905–909.
- (61) Yin, L.; Castagnino, P.; Assoian, R. K. ABCG2 expression and side population abundance regulated by a transforming growth factor beta-directed epithelial-mesenchymal transition. *Cancer Res.* **2008**, *68*, 800–807.

## Abbreviations Used

HPPH, 2-[1-hexyloxyethyl]-2-devinyl pyropheophorbide-a; ALA, aminolevulinic acid; ABC, ATP-binding cassette; CSC, cancer stem cells; IM, imatinib mesylate; PhA, pheophorbide-a; PPA, pyropheophorbide-a; PDT, photodynamic therapy; PS, photosensitizer(s); PpIX, protoporphyrin IX; SP, side population; SCLCC, stem cell-like cancer cells; TIC, tumor initiating cells.

**Acknowledgment.** We thank Dr. Susan Bates (NIH) for the gift of ABCG2 positive HEK-293 482R and ABCG2 negative HEK-293 PcDNA cells, Earl Timm (RPCI) for assistance with flow cytometry and Dr. David Bellnier (RPCI) for helpful criticism of the manuscript. This work was supported by NIH grant CA55791 and the shared resources of the Roswell Park Cancer Center support grant CA16056; and the training grant C023075 from the NYS-TEM initiative.

**Supporting Information Available:** Additional figures as noted in the text. This material is available free of charge via the Internet at <http://pubs.acs.org>.

MP100154J